AIAA JOURNAL
Vol. 48, No. 7, July 2010

Modified Dynamic Preisach Model for Hysteresis

Mohammed R. Sunny* and Rakesh K. Kapania†
Virginia Polytechnic Institute and State University, Blacksburg, Virginia 24061

DOI: 10.2514/1.J050189

A dynamic hysteresis model developed by modifying the relay operator in the classical Preisach model and adding a dynamic relaxation operator to simulate the change in electrical resistance with strain in conductive polymer nanocomposites is proposed. Data from the conductivity test on a conductive polymer nanocomposite sample are presented to show the hysteretic variation of electrical resistance with strain. A hysteresis model developed by modifications on the relay operators and addition of a dynamic relaxation operator is described. Effectiveness of the model in simulating the behavior of conductive polymer nanocomposites is explained. A modal function based identification procedure to determine the parameters associated with the model is described. Efficiency of the model is discussed by comparison of the result obtained from the model with the experimental result.

Nomenclature

f = output
h = dynamic relaxation operator
R = electrical resistance
u = input
α = upswitching value of each relay operator
β = downswitching value of each relay operator
γ = relay operator in Preisach model
ϵ = strain
ζ = upswitching value of each dynamic relaxation operator
η = downswitching factor associated with each relay operator
μ = weight associated with each relay operator

I. Introduction

HYSTERESIS represents a property of systems that show dependence on input history applied to it (i.e., output at any time instant depends on the input applied to the system both at the present time as well as the previous history); consequently, the same instantaneous value of the input can give different outputs, depending on input history. Hysteretic phenomena are encountered in various branches of engineering, such as magnetic hysteresis, electrical hysteresis, ferroelectric hysteresis, electron beam hysteresis, adsorption hysteresis, etc. Viscoelastic behavior of composite laminates [1,2] and rheological behavior of polymers are other well-known examples of hysteretic behavior [3].

Different mathematical models have been developed, depending on the type of hysteretic behavior and successfully applied in these fields. Strain-resistance behavior in conductive polymers is an important property that requires a proper hysteresis model for its characterization. Conductive polymer nanocomposite materials have high electrical conductivity and low elastic modulus. Their sheet resistance is 0.1–100 Ω/sq. and can undergo strain up to 200–300%. These materials can be used as a possible sensor to measure large strain in inflatable structures, such as tires. Our research has been motivated by our need to use conductive polymer nanocomposites for large-strain sensing. The main features observed in the hysteresis loop formed by the variation of the electrical resistance with strain in conductive polymer nanocomposites are that the loop keeps shifting up with change in the width of the loop with number of cycles and relaxation, i.e., decay of output, occurs at any constant value of input. Because of the phenomenon of relaxation, the value of input depends on the input history as well as the history of the rate of application of input. Because of this rate-dependent nature, the hysteresis has been referred to as dynamic hysteresis in this paper.

Hysteresis models are either physics-based or empirical. Physics-based models, being mainly microscopic and semimicroscopic, involve application of energy principle and thermodynamic, electromagnetic, or other laws, depending on type of the problem at the grain level [4]. The main disadvantage with such models is the requirement of a large number of material parameters. Our goal is to develop a mathematical model to solve the forward problem: i.e., to simulate the variation of electrical resistance with strain in the sensor. After that, we want to develop a compensator using the model to solve the inverse problem: i.e., to remove the effect of hysteresis and relaxation from output obtained from the sensor to facilitate the calibration of the sensor. We are more interested in empirical models, which require fewer parameters and are suitable for practical applications. We first reviewed two of the several existing hysteresis models: namely, the fractional calculus and Preisach models. We found that both these approaches in their traditionally used forms did not lend their application to our data readily.

Fractional calculus allows the definition of derivative and integral of a function of any generalized order. This approach has proven to be very effective in modeling the dynamic behaviors of different kinds, especially of viscoelastic materials showing hysteresis coupled with relaxation. Nutting [5] observed that stress relaxation could be modeled by fractional powers of time. This can be viewed as the progenitor of fractional calculus approach of modeling viscoelastic behavior [6]. Li and Xu [7] showed the use of fractional calculus to model the hysteresis and precondition in viscoelastic solids. Application of a modified version of the fractional calculus approach to model the hysteresis and relaxation in the variation of electrical resistance with strain in conductive polymer nanocomposite materials can be found in the previous work by the authors [8]. In this paper, we propose a modified Preisach model to represent the path-dependent behavior of conductive polymers.

In 1935 Preisach [9] developed the well-known model to represent path-dependent behavior of magnetic materials based on some plausible hypothesis concerning the physical mechanisms of magnetism. In this model the hysteresis is considered as a weighted combination of the outputs from a numbers of elementary hysteresis operators, called relay operators. Everett and Whitton [10] independently invented and developed the model for adsorption hysteresis. Later, several modifications were proposed to take care of dependence of output on rate of input, stabilization process, etc. Cornejo and Missell [11] used the Preisach model to model nanocrystalline magnets. Roshko and Huo [12] characterized the irreversible response of a ferromagnet pervoskite ($SrRuO_3$) with a Curie temperature 160 K. Vandenbossche et al. [13] investigated the application of

Received 4 September 2009; revision received 26 November 2009; accepted for publication 3 February 2010.

*Ph.D. Candidate, Department of Aerospace and Ocean Engineering, Sensors and Structural Health Monitoring Group; sunny@vt.edu.
†Mitchell Professor, Department of Aerospace and Ocean Engineering; rkapania@vt.edu. Associate Fellow AIAA.

magnetic hysteresis measurement combined with Preisach model for the evaluation of fatigue damage progression. Determination of the weight function and very high computation time were found to be major problems in using Preisach model. Guyer et al. [14] described the use of simulated annealing, normal mode analysis and exponential decay to solve these problems and showed a comparison among the performance of these approaches. Schiffer and Ivanyi [15] showed the use of wavelets to determine the weights used in the Preisach model. The weight functions were derived for some operators and two-dimensional wavelet average interpolation transform was applied to interpolate the function for other operators. Yunhe et al. [16] represented system outputs and Preisach function by wavelet approximation.

A dynamic rate-dependent Preisach model can be found in Mayergoyz [17]. It assumes the distribution of weight functions associated with each relay operator to be dependent on the current value of the output $f(t)$. This ultimately leads to an expression for the output $f(t)$ having two parts: the rate-dependent part $f_d(t)$ and the static part $f_s(t)$. If the input reaches a value $u(t_0)$ at time instant t_0 and is kept constant at that value, the output starts relaxing from time instant t_0. The relaxation follows an exponential relation with time, as shown below:

$$f_d(t) = (f(t_0) - f_s(t))e^{-(t-t_0)/\tau} \tag{1}$$

Here, $f(t_0)$ is the value of total output at time instant t_0. The factor τ controls the rate of relaxation. Use of this approach to model the dynamic hysteresis can be found in Cross et al. [18]. According to this dynamic model, both $f_0(t)$ and τ depend upon the weights associated with relay operators. Hence, compensation of hysteresis and relaxation becomes computationally complex. Here, we propose a model which considers static hysteresis and relaxation to be an independent phenomenon. A modified relay operator capable of taking care of upward movement of hysteresis loop after each cycle is proposed first. Next, we propose a dynamic relaxation operator that is independent of the relay operators. A combination of the outputs from the static relay operators and the dynamic relaxation operators give rise to hysteresis with relaxation. A mathematical model of a compensator based on our proposed model can be found in [19]. First, experiments carried out on a conductive polymer nanocomposite sample to study the variation of electrical resistance with strain applied to it are described in this paper. A brief description of the Preisach model is given next. Then the modifications needed to model our experimental data and associated identification procedure are explained. Results from the proposed model are compared with the experimental data and concluding remarks are made.

II. Experimental Details

A conductivity test was carried out on a conductive polymer nanocomposite sample to study the variation of electrical resistance with strain in it. The experimental setup used for this test is shown in Fig. 1. The sample was clamped at the two ends of the linear stage (NLS4-10-25 by Newmark Systems, Inc.). The top clamp of the linear stage is fixed. The bottom clamp can move and apply a strain to the material at a desired rate. Movement of the bottom clamp can be controlled by IMS Lynx Terminal, a software provided by Intelligent Motion Systems, Inc. This helps us to apply strain to the material with a desired rate. The two ends of the sample close to the clamps are connected to a 46-range digital multimeter with an interface to a computer through serial port (RS-232). The multimeter shows the electrical resistance of the portion of the material between the connected ends. Readings of the multimeter are stored in a computer through a program Meterview 1.0, provided by RadioShack. Using this setup, a time-dependent strain can be applied to the sample and its electrical resistance can be measured at different time instants at different strain levels. A time-dependent cyclic strain input, as shown in Fig. 2a with strain rate $0.15\%/\mathrm{s}$ was applied to the system and the resulting time-dependent resistance was measured. Change in output resistance with input strain and time is shown in Fig. 3a and 3b. Output obtained from the experiment contained a high frequency noise which was removed by using a low-pass filter to smooth the experimentally obtained curve. In Figs. 3a and 3b, the unfiltered and the smoothed (filtered) data are presented. The smoothed data obtained after performing two sets of experiments are shown to ensure the repeatability of the experiment.

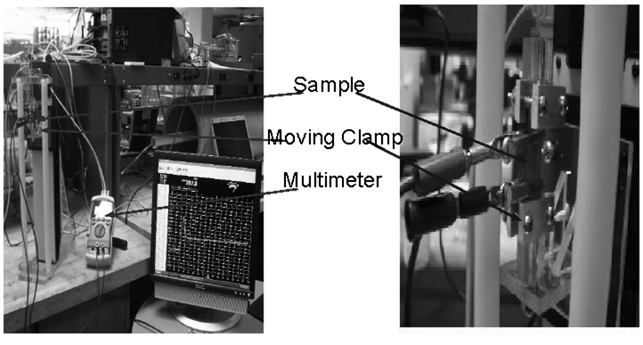

Fig. 1 Experimental setup.

The smoothed data obtained from first experiment are used later for developing the mathematical model. Let us term this data set as data set 1. After this, the material was allowed to relax and another experiment was performed by applying a strain, as shown in Fig. 2b with a higher strain rate ($0.3\%/\mathrm{s}$). The result obtained from this experiment is shown in Fig. 3c. Let us call it data set 2. Data set 2 has been used to evaluate the model.

III. Preisach Model

The Preisach model considers the hysteresis loop to be a weighted combination of output from different independent relay operators. Each independent operator $\gamma_{\alpha\beta}$ is a mechanical unit that upswitches to a value $+1$ when the value of input u is α and is increasing and downswitches to a value -1 when the value of input u is β and is decreasing. Definition of the operator is given in Eq. (2). Here, α and β are called up- and downswitching values, respectively. It will be assumed subsequently that $\alpha \geq \beta$, which is quite natural from the physical point of view [17]. Figure 4 shows the behavior of $\gamma_{\alpha\beta}$. The ascending branch $abcde$ is followed when the input increases monotonically and the descending branch $edfba$ is followed when the input decreases monotonically. According to this model, output $f(t)$ is given by Eq. (4):

$$\gamma_{\alpha\beta}[u](t) = \begin{cases} +1 & \text{for } u(t) \geq \alpha \\ -1 & \text{for } u(t) \leq \beta \\ \gamma_{\alpha\beta}[u](0) & \text{for } u(t) < \alpha \& u(t) > \beta \end{cases} \tag{2}$$

$$f[u](t) = \int_{T_1} \mu(\alpha, \beta)\, \mathrm{d}\alpha\, \mathrm{d}\beta - \int_{T_2} \mu(\alpha, \beta)\, \mathrm{d}\alpha\, \mathrm{d}\beta \tag{3}$$

Figure 5 shows the geometric interpretation of the Preisach model. The space spanned by α and β is called Preisach–Mayergoyz (PM) (after Preisach [9] and Mayergoyz [20]) space [14]. ΔABC is the region where $\alpha \geq \beta$. This is the feasible region of PM space. The input protocol leads to a trajectory separating the PM space into upswitched and downswitched regions, as shown in Fig. 5. T_1 and T_2 refer to the regions where operators are in upswitched and downswitched states, and T refers to the region containing all the operators. Depending on input history, T_1 and T_2 change. According to Eq. (3), the values of the input depend on the input history only. Rate of change of input does not affect the value of output.

At the beginning of the cycle, all the operators are in downswitched state, as shown in Fig. 5a. Output f_1 at this stage can be calculated using Eq. (4). When input reaches a value u, output f_2 is given by Eq. (5). Figure 5b shows the regions where the operators are at upswitched and downswitched state. At the end of the first half of the cycle, all the operators come to the upswitched state. Equation (6) shows the value of output and Fig. 5c shows the PM space. Now, after the input starts decreasing monotonically and reaches a value u

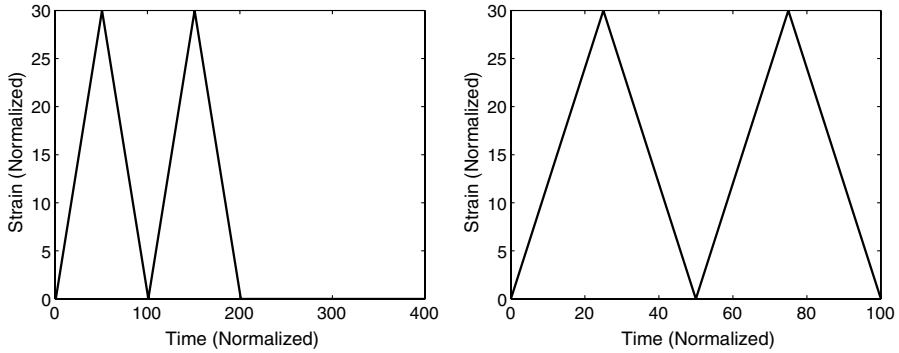

a) Strain vs time (data set-1) **b) Strain vs time (data set-2)**

Fig. 2 Applied strain and its history.

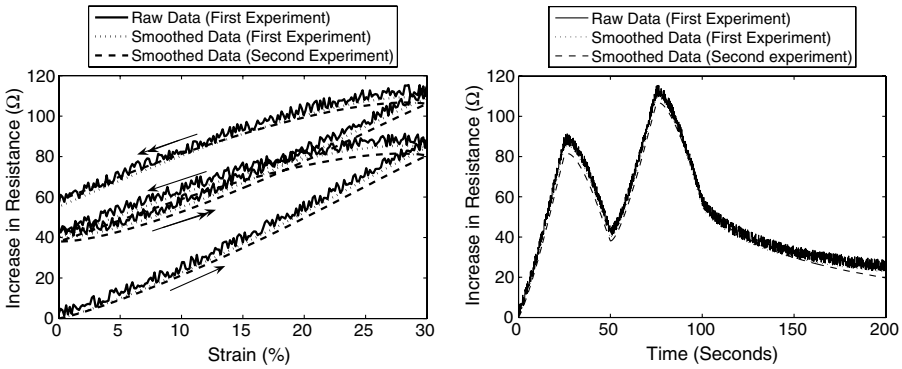

a) Resistance vs strain (data set-1) **b) Resistance vs time (data set-1)**

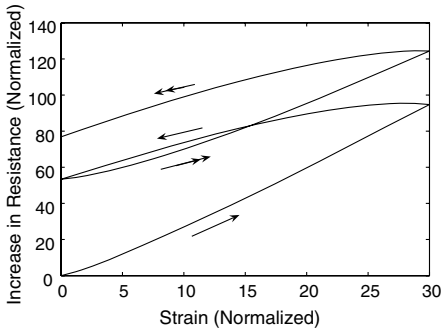

c) Resistance vs strain (data set-2)

Fig. 3 Experimental results.

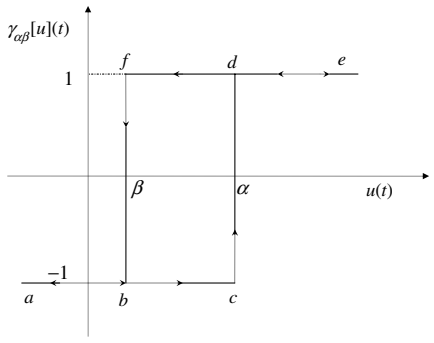

Fig. 4 Relay operator in the classical Preisach model.

again, the output reaches a value f_4, as shown in Eq. (7). Regions with upswitched and downswitched operators in the PM space are shown in Fig. 5d. Comparison of Figs. 5b and 5d shows that when the input increases monotonically, the operators in the region ABCD is in downswitched state at u and the operators in the same region remains in upswitched state at the same value of input when the input decreases monotonically. This creates a difference in output $f_4 - f_2$ as given in Eq. (8) and causes the hysteresis. At the end of the cycle all the operators go back to the downswitched state and the output returns to its initial value. In this way in a complete cycle this model gives rise to a closed-loop hysteresis. Wiping out and congruent minor loop properties are two important properties completely characterizing a classical Preisach hysteresis loop. According to the wiping-out property, each input extremum having a value u_1 wipes out the effect of previous extremum of value u_2 if $|u_1| > |u_2|$. According to the congruency of minor loops, all the minor loops generated under monotonically varying inputs of identical amplitudes are identical in shape. A detailed discussion of these properties can be found in Mayergoyz [17]. A discussion on piecewise monotony and continuity can be found in Tan and Bennani [21]. Equations showing the value of the output at different stages of the cycle are as follows:

$$f_1 = \int_{\mathrm{ABC}} -\mu(\alpha, \beta)\, \mathrm{d}\alpha\, \mathrm{d}\beta \tag{4}$$

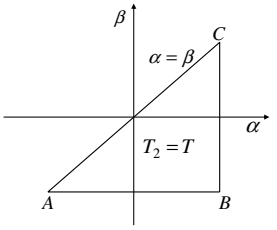

a) At the beginning of the cycle

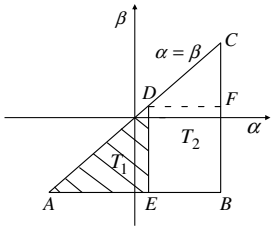

b) During the first half of the cycle when input increases monotonically and reaches a value u

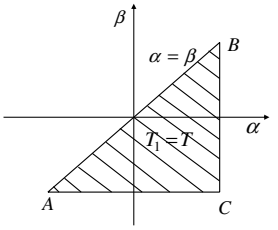

c) At the end of the first half of the cycle

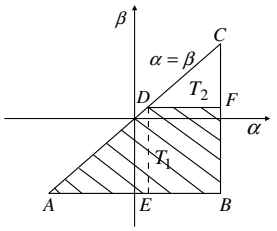

d) During the second half of the cycle when input decreases monotonically and reaches a value u

Fig. 5 PM space at different stages of the first cycle.

$$f_2 = \int_{\text{AED}} \mu(\alpha, \beta)\, \mathrm{d}\alpha\, \mathrm{d}\beta - \int_{\text{EBCD}} \mu(\alpha, \beta)\, \mathrm{d}\alpha\, \mathrm{d}\beta \tag{5}$$

$$f_3 = \int_{\text{ABC}} \mu(\alpha, \beta)\, \mathrm{d}\alpha\, \mathrm{d}\beta \tag{6}$$

$$f_4 = \int_{\text{ABFD}} \mu(\alpha, \beta)\, \mathrm{d}\alpha\, \mathrm{d}\beta - \int_{\text{CDF}} \mu(\alpha, \beta)\, \mathrm{d}\alpha\, \mathrm{d}\beta \tag{7}$$

$$f_4 - f_2 = 2 \int_{\text{DEBF}} \mu(\alpha, \beta)\, \mathrm{d}\alpha\, \mathrm{d}\beta \tag{8}$$

IV. Development of the Modified Preisach Model

The relay operator described in the previous section gives rise to a closed-loop hysteresis in a complete cycle and cannot model relaxation of output at a constant input. In our model, upward shifting of the hysteresis loop has been taken care of by a modification of the relay operator and relaxation has been taken care of by the addition of a dynamic operator, defined subsequently. The static part of the output obtained from the modified relay operators is termed as the static part of the output (f_s) and the dynamic part of the output obtained from the dynamic operators is termed as the dynamic part of the output (f_d). Total output from the system is the combination of f_s and f_d.

A. Modification of the Relay Operator

For our problem, both the input strain and the output electrical resistance always remain positive. So, α, β and output from each operator $\gamma_{\alpha\beta}$ always remain positive. Hence, in the downswitched state, output from each operator is zero. The relay operator considered in our model is shown in Fig. 6. Output of this operator does not depend on rate of change of input. Here, at $u = \alpha$, the operator upswitches by a value $+1$. But at $u = \beta$, it does not downswitch fully. It downswitches by a value η, which is an another parameter associated with each relay operator. Because of this partial downswitching at β, the loop keeps shifting upward with the number

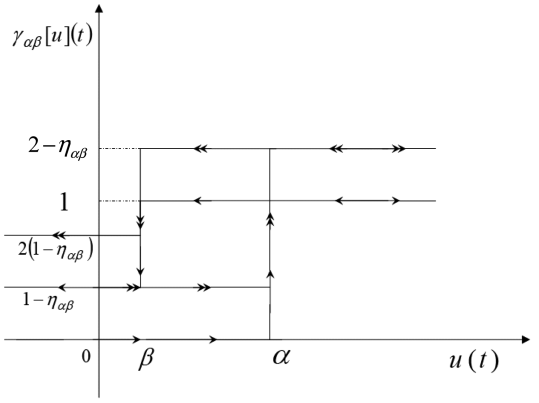

Fig. 6 Proposed relay operator in modified Preisach model.

of cycles, as shown in Fig. 6. If the value of η is more than 1, the loop will shift downward. As the operators do not downswitch fully, at any time instant, an operator can be either fully downswitched, upswitched, or partially downswitched, depending on the input history. The partially downswitched state refers to the state of the operator after it downswitches by η followed by any upswitching. It can be called partially upswitched state also. Output of an operator at partially downswitched state after n number of upswitchings and partial downswitchings will be $n(1-\eta)$ and of an operator at upswitched stage after n number of upswitchings and partial downswitchings will be $n(1-\eta)+1$. The relay operator in the classical Preisach model retains its congruency of minor loops, piecewise monotony and continuity after the proposed modification. However, as each cycle of input results in upward shifting of the hysteresis loop, extremum having a value u_1 does not wipe out the effect of previous extremum of value u_2 if $|u_1| > |u_2|$:

$$f_s[u](t) = \int_{T_1} (n(\alpha, \beta)(1 - \eta(\alpha, \beta)) + 1)\mu(\alpha, \beta)\, \mathrm{d}\alpha\, \mathrm{d}\beta + \int_{T_3} n(\alpha, \beta)(1 - \eta(\alpha, \beta))\mu(\alpha, \beta)\, \mathrm{d}\alpha\, \mathrm{d}\beta \tag{9}$$

where T_3 refers to the regions where all the operators are in partially downswitched state.

Figure 7 describes the states of the operators in the PM space during different stages of a cycle. Equations (7–13) show the value of output at these stages. At the beginning of the first cycle, the output is zero, as all the operators are in the downswitched state. When the input increases monotonically and reaches a value u, the output is given by Eq. (7). States of different operators in PM space at this stage is shown in Fig. 7a. Figure 7b and Eq. (11) show the state of operators and the value of the output at the end of the first cycle. When the input starts decreasing some operators start downswitching partially, as shown in Fig. 7c. Equation (12) shows the value of the output at this stage when the value of the input is u. At the end of the cycle all the operators come to a partially downswitched state, as shown in Fig. 7d. Output at this stage can be calculated using Eq. (13). Equations (7) and (12) show that same value of input u gives different values of output due to differences in input history. This is due to the memory effect associated with the relay operators that result in the hysteresis:

$$f_{s_2} = \int_{\text{AED}} \mu(\alpha, \beta)\, \mathrm{d}\alpha\, \mathrm{d}\beta \tag{10}$$

$$f_{s_3} = \int_{\text{ABC}} \mu(\alpha, \beta)\, \mathrm{d}\alpha\, \mathrm{d}\beta \tag{11}$$

$$f_{s_4} = \int_{\text{ABFD}} \mu(\alpha, \beta)\, \mathrm{d}\alpha\, \mathrm{d}\beta + \int_{\text{DFC}} (1 - n(\alpha, \beta))\mu(\alpha, \beta)\, \mathrm{d}\alpha\, \mathrm{d}\beta \tag{12}$$

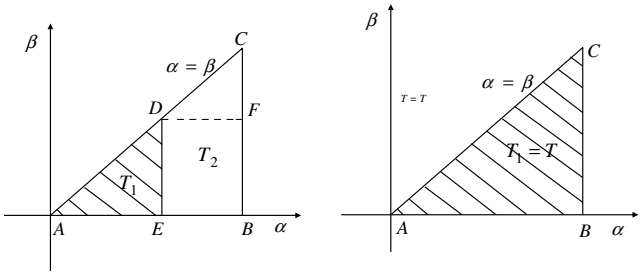

a) During the first half of the cycle when input increases monotonically and reaches a value *u*

b) At the end of the first half of the cycle

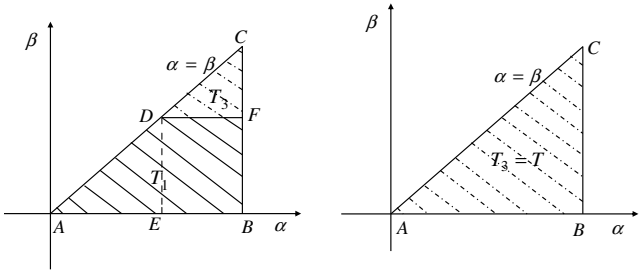

c) During the second half of the cycle when input decreases monotonically and reaches a value *u*

d) At the end of the cycle

Fig. 7 PM space at different stages of the first cycle.

$$f_{s_5} = \int_{\text{ABC}} (1 - n(\alpha, \beta))\mu(\alpha, \beta)\, \mathrm{d}\alpha\, \mathrm{d}\beta \tag{13}$$

In this way, a partial downswitching causes a difference between the outputs at the end and beginning of the cycle. Consequently, the hysteresis loop keeps shifting upward. This is the advantage of using this operator in modeling the hysteresis showing upward movement with number of cycles. The classical Preisach model is a special case of this modified version where the downswitching factor of each relay operator is 1. Like the classical Preisach model, this modified Preisach model also cannot take care of dependence output on input rate.

B. Addition of a Dynamic Operator

In this section, a dynamic relaxation operator is introduced to take care of relaxation and input rate dependence. The dynamic part of the output is assumed to be the result of dynamic relaxation operators. Relaxation is a time-dependent phenomenon. Hence, the dynamic relaxation model introduced in this section is a function of time. These operators have upswitching value ζ, but no downswitching value. When the input monotonically increases and reaches a value ζ, an operator h_ζ upswitches to a value

$$\sum_{j=1}^{P} A_j$$

and then decays exponentially as given in Eq. (14). Here, $A_j(\zeta)$, $b_j(\zeta)$, and $c_j(\zeta)$ $(j = 1, \ldots, P)$ are unknown parameter associated with each dynamic operator. These need to be determined from experimental data. As t approaches infinity, output of the dynamic relaxation operator approaches zero, signifying a full relaxation. The dynamic relaxation operators lie on a one-dimensional space spanned by ζ. Hence, for a given input history at time t, the dynamic part of the output will be given by Eq. (15):

$$h_\alpha(t) = \begin{cases} 0 & \text{if } t < t_0 \\ \sum_{j=1}^{P} A_j e^{-b_j(t-t_0)^{c_j}} & \text{if } t \geq t_0 \end{cases} \tag{14}$$

$$f_d(t) = \int_{T_d} \sum_{i=1}^{n_\alpha} \sum_{j=1}^{P} A_j e^{-b_j(t-t_{\zeta i})^{c_j}}\, \mathrm{d}\alpha \tag{15}$$

Here, T_d refers to the domain where the operators are in the upswitched state. It depends upon the input history. n_ζ refers to the total number of times h_ζ was upswitched and $t_{\zeta i}$ refers to the time instant at which h_ζ was upswitched for the ith time. Total value of the output from the system is the combination of static and dynamic part of the output obtained from Eqs. (9) and (15).

V. Numerical Implementation

In this section, a numerical technique to calculate the static and dynamic part of the output using the modified Preisach model described in the previous section is explained. Calculation of the static part of the output f_s involves evaluation of area integral in the space of the relay operators. To simplify the evaluation of the area integral, the PM space is assumed to consist of different bins $B_{ij}(i = 1, N; j = 1, i)$, as shown in Figs. 8 and 9. Parameters μ and η have uniform values throughout the area in each bin. Bins of finer size improve the accuracy of the model. Let us suppose that the input starts increasing monotonically from zero. At time step t_{i-1}, the values of input and output are u_{i-1} and f_{i-1}, respectively. At this time, all the relay operators in the domain T_{i-1}, as shown in Fig. 8 are in the upswitched state. At the next time step t_i, when the input reaches a value u_i, operators in the domain T_i come to the upswitched state. The output at this time step can be calculated as

$$f_s(t_i) = f_s(t_{i-1}) + \sum_{k=1}^{N_{\Delta T}} \mu_k A_{rk} \tag{16}$$

Here, $N_{\Delta T}$ is the total number of bins in domain ΔT, as shown in Fig. 8. (bins with a dot in the center) in Fig. 9. Parameter μ_k represents the weight functions associated with the relay operators in the kth bin, and A_{rk} is the area of the kth bin.

Let us suppose that after reaching a value u_m, the input starts decreasing monotonically. In Fig. 9, T_{i-1} and T_i are the domains containing relay operators in upswitched state for values of input u_{i-1} and u_i, occurring at two consecutive time steps t_{i-1} and t_i. Output at time step t_i can be calculated as

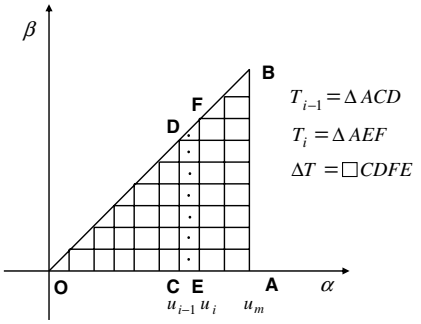

Fig. 8 PM space at t_i and t_{i-1} when the input is increasing.

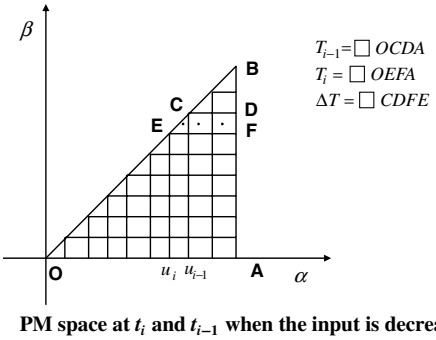

Fig. 9 PM space at t_i and t_{i-1} when the input is decreasing.

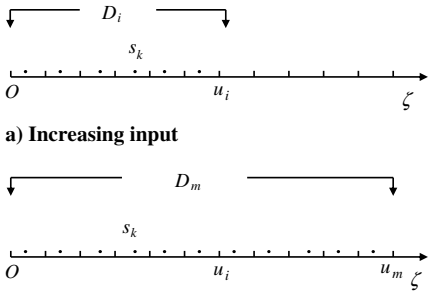

a) Increasing input

b) Decreasing input

Fig. 10 Space of dynamic relaxation operators.

$$f_s(t_i) = f_s(t_{i-1}) - \sum_{k=1}^{N_{\Delta T}} \eta_k A_{rk} \tag{17}$$

where η_k is the value of downswitching values associated with the relay operators in the kth bin in the domain ΔT, and $N_{\Delta T}$ is the total number of bins in domain, as shown in Fig. 9.

For calculation of the dynamic part of the output f_d, the 1-D space containing the dynamic relaxation operators is assumed to consist of different line segments. $A_i (i = 1, \ldots, P)$, defined in the previous section, have uniform values throughout the length of each segment. At time step t_i, when the input reaches value u_i after starting to increase monotonically from a value of zero, operators in the domain D_i (containing segment with dots in Fig. 10a) are in a state of relaxation followed by an upswitching. If the input reaches a value u_l at time step t_l, then the value of the output from the operator with upswitching value u_l at time step t_i will be

$$h_{u_l}(t_i) = \sum_{j=1}^{P} A_j e^{-b_j (t_i - t_l)^{c_j}} \tag{18}$$

If we assume the size of the segments to be very small, then we can write the total output from all the operators in the segment S_n, containing the operator h_{u_l} to be

$$S_n(t_i) = \sum_{j=1}^{P} A_j e^{-b_j (t_i - t_l)^{c_j}} L_n \tag{19}$$

where L_n is the length of segment n. Hence, the total value of the dynamic part of the output at time instant t_i will be

$$f_d(t_i) = \sum_{k=1}^{N_{D_i}} S_k(t_i) \tag{20}$$

where N_{D_i} is the total number of segment in the domain D_i.

If the input reaches a value u_m, operators in the segments D_m, shown in Fig. 10 (containing dots at the center) comes to a state of relaxation followed by upswitching. After that if the input starts decreasing all the operators in domain D_m keeps relaxing. Hence, at t_i, when the input reaches a value u_i while decreasing monotonically from u_m, dynamic part of the output can be written as

$$f_d(t_i) = \sum_{k=1}^{N_m} S_k(t_i) \tag{21}$$

where N_{D_m} is the total number of segment in domain D_m, and $S_k (k = 1, \ldots, N_{D_m})$ can be calculated using the Eqs. (18) and (19).

VI. Identification of Parameters

The objective of the present research is to identify parameters in the model from the experimental data. In our case, strain $\epsilon(t)$ is the input $u(t)$ and electrical resistance $R(t)$ is the output $f(t)$. Unknown material parameters can be found by minimizing the error of the output predicted by the mathematical model with respect to the experimental data. Before that, some assumptions are made regarding parameters associated with the hysteresis and dynamic operators. For the hysteresis operators, the value of μ and η in bin $B_{i,j}$ is assumed to be a combination of M numbers of different modal functions, as shown in Eqs. (22) and (23):

$$\mu(i, j) = \sum_{l=1}^{M} b_{\mu_l} \phi_{\mu_l}(i, j) \tag{22}$$

$$\eta(i, j) = \sum_{l=1}^{M} b_{\mu_l} \phi_{\eta_l}(i, j) \tag{23}$$

The lth modal functions ϕ_{μ_l} and ϕ_{η_l} are given by the following equations:

$$\phi_{\mu_l}(i, j) = \cos\left(\frac{\pi m_{\mu_l} i}{N}\right) \cos\left(\frac{\pi n_{\mu_l} j}{N}\right) + \cos\left(\frac{\pi n_{\mu_l} i}{N}\right) \cos\left(\frac{\pi m_{\mu_l} j}{N}\right) \tag{24}$$

$$\phi_{\eta_l}(i, j) = \cos\left(\frac{\pi m_{\eta_l} i}{N}\right) \cos\left(\frac{\pi n_{\eta_l} j}{N}\right) + \cos\left(\frac{\pi n_{\eta_l} i}{N}\right) \cos\left(\frac{\pi m_{\eta_l} j}{N}\right) \tag{25}$$

Hence, $\mu(i, j)$ is a function of unknown parameters b_{μ_l}, m_{μ_l}, and n_{μ_l}, and $\eta(i, j)$ is a function of unknown parameters b_{η_l}, m_{η_l}, and n_{η_l} $(l = 1, \ldots, M)$. Details of this modal function based identification procedure can be found in Guyer et al. [14].

Parameter $A_j(\zeta)$ for the operators in the ith segment of the space of relaxation operators is assumed to be of the form $A_j = a_j i^{d_j}$ $(j = 1, \ldots, P)$, and $b_j(\zeta)$ and $c_j(\zeta)$ are assumed to be same for all the segments. So, unknown parameters associated with the dynamic part of the model are $a_j(\zeta)$, $b_j(\zeta)$, $c_j(\zeta)$, and $d_j(\zeta)$ $(j = 1, \ldots, P)$.

By using all these assumptions, electrical resistance can be written as a function of the parameters b_{μ_l}, m_{μ_l}, n_{μ_l}, b_{η_l}, m_{η_l}, n_{η_l}, a_j, b_j, c_j, and d_j $(l = 1, \ldots, M;\ j = 1, \ldots, P)$. By finding the values of these parameters, the material can be characterized. Now an error function can be defined as

$$E = \sum_{i=1}^{N} (R_e(i) - R_c(i))^2 \tag{26}$$

Here, $R_e(i)$ is electrical resistance obtained from experiment and $R_c(i)$ is the electrical resistance obtained from the proposed model (using the assumptions described above) at the ith data point. By minimizing this error, the unknown parameters were found.

We used two identification schemes. In scheme 1, unknown parameters associated with the model were estimated by minimizing the sum of the squares of errors E in the time interval of [0, 200] s (considering the cyclic variation of resistance with cyclic strain only) of data set 1.

In scheme 2, separate minimizations were carried out to find the parameters associated with dynamic and static part of the model. At first, we considered the data in the interval of [201, 400] s (considering the relaxation only) in data set 1. At this interval, strain is kept at a constant value (30%). Hence, output electrical resistance has the dynamic part (R_d) only. By minimizing the sum of the squares of differences of R_d predicted by the model and obtained from the experiment, unknown parameters associated with the dynamic part of the model were found. After that, using these parameters dynamic part of the output R_d in the interval of [0, 200] s (considering the cyclic variation of resistance with cyclic strain only) were found. Subtraction of R_d from the total value of electrical resistance obtained from experiment gives the static part of output R_s in the interval of [0, 200] s. By minimizing the sum of the squares of the difference between R_s predicted by the model and R_s obtained from the experiment, unknown parameters associated with the static part of the model were determined.

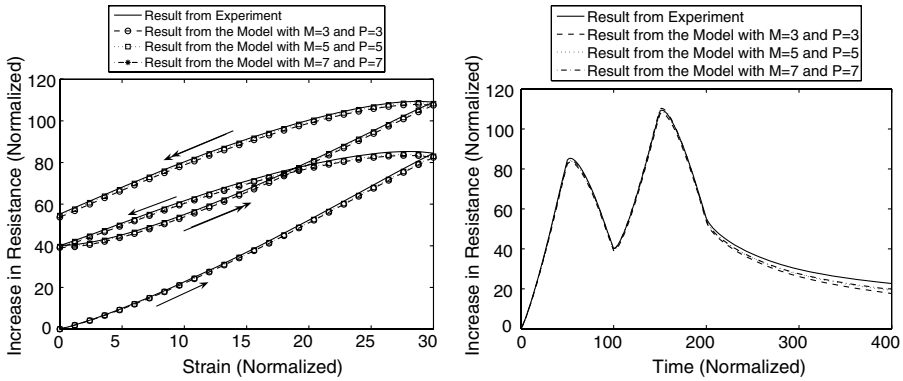

a) Resistance vs strain **b) Resistance vs time**

Fig. 11 Comparison of the results from the model with the experimental result (data set 1).

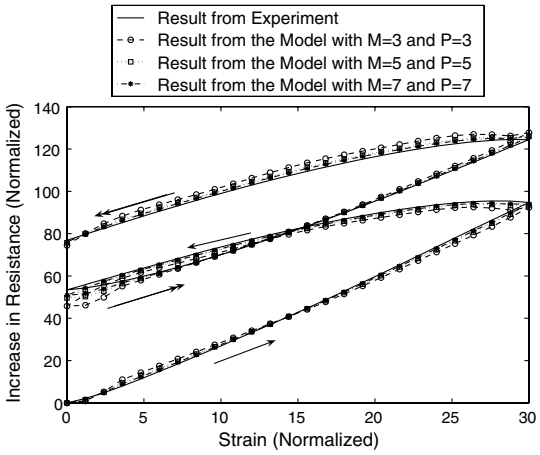

Fig. 12 Comparison of the results from the model with the experimental result (data set 2).

VII. Conclusions

Parameter estimation was done by assuming different values of M (number of modal functions for the distribution of $\mu(\alpha, \beta)$ and $\eta(\alpha, \beta)$ in the PM space) and P (number of exponential functions for the dynamic operators h_ζ) to observe the improvement of results with an increase in number of parameters. The error minimization was carried out by using the function `fmincon` in MATLAB using a personal computer (Dell Precision PWS690) with 2.66 GHz processor speed and 2 GB RAM. At first, unknown parameters associated with the model were estimated by using the identification scheme 1. Using these parameters, the change in electrical resistance was found in the time interval of [0, 400] s. Figures 11a and 11b show the change in the electrical resistance with strain and time, respectively, for the type of strain input in data set 1. Corresponding errors and CPU times are tabulated in Table 1. After that using the same parameters variation of electrical resistance for input in data set 2 was determined. Results are shown in Fig. 12. Table 1 shows the corresponding errors. Comparison with experimental data set 1 shows that the model is appropriate enough to simulate the path-dependent behavior of these materials for that strain rate. An increase in the number of modal functions for the distribution of $\mu_0(\alpha, \beta)$, $\mu_1(\alpha, \beta)$, and $\eta(\alpha, \beta)$ in the PM space and number of exponential functions for the dynamic operators h_ζ results in an improvement of the results. Parameters determined by minimizing the error in the time interval of [0, 200] s of data set 1 predict the relaxation in the time interval of [200, 400] s accurately, as shown in Fig. 11b. Figure 12, showing the comparison with experimental data set 2 obtained by applying a time-dependent strain with a higher strain rate, shows that the model is robust enough to take care of input rate dependence.

Table 1 Error and CPU time corresponding to different values of M and P (identification scheme 1)

M	P	% error (data set 1, data set 2)	CPU time for error minimization, s
3	3	2.40, 4.10	1259
5	5	1.91, 2.50	1715
7	7	1.08, 2.10	2710

Table 2 Error and CPU time corresponding to different values of M and P (identification scheme 2)

M	P	% error (data set 1, data set 2)	CPU time for error minimization, s
3	3	2.20, 4.00	1001
5	5	1.81, 2.29	1322
7	7	1.03, 2.01	2143

Using the parameters obtained using identification scheme 2, unknown parameters were calculated. We next considered the data in the interval of [201,400] s (considering the relaxation only) in data set 1. Table 2 shows the errors and total CPU times for different values of M and P. It can be seen that the errors in Tables 1 and 2 are almost same, but the CPU times are significantly lower in Table 2. This is due to the fact that separate minimizations for the dynamic and static part of the model reduces the number of the unknown variables associated with each minimization.

In this paper, a modified version of the Preisach model, the associated identification procedure, and its use in modeling the hysteresis shown by conductive polymer nanocomposites are described. Introduction of the partial downswitching to the relay operators makes the model flexible enough to simulate the upward shifting of the hysteresis loop with numbers of cycles. Addition of the dynamic operator helps to take care of the relaxation phenomena. Comparison with the experimental result proves the efficiency of the model. The sensor has to be calibrated for its use using this model. Applicability of this model needs to be verified for others materials (electroactive polymers such as dielectric elastomers and ionic polymer metal composites) showing hysteresis and relaxation.

Acknowledgments

The research was performed under project grant NNL05AA29G from NASA Langley Research Center (LaRC) and by the Institute for Critical Technologies and Sciences (ICTAS) at Virginia Polytechnic Institute and State University. The authors would like to acknowledge Nakhiah C. Goulboune, Department of Mechanical Engineering at Virginia Polytechnic Institute and State University, for her guidance in carrying out the experiments.

References

[1] Hammerand, D. C., and Kapania, R. K., "Thermo-Viscoelastic Analysis of Composite Structures Using a Triangular Flat Shell Element," *AIAA Journal*, Vol. 37, No. 2, 1999, pp. 238–247. doi:10.2514/2.696

[2] Hammerand, D. C., and Kapania, R. K., "Geometrically Nonlinear Shell Element for Hygrothermorrheologically Simple Linear Viscoelastic Composites," *AIAA Journal*, Vol. 38, No. 12, Dec. 2000, pp. 2305–2319. doi:10.2514/2.900

[3] Heymans, N., "Constitutive Equations for Polymer Viscoelasticity Derived from Hierarchical Models in Cases of Failure of Time-Temperature superposition," *Signal Processing*, Vol. 83, No. 11, Nov. 2003, pp. 2345–2357. doi:10.1016/S0165-1684(03)00187-7

[4] Viswamurthy, S. R., and Ganguli, R., "Modeling and Compensation of Piezoceramic Actuator Hysteresis for Helicopter Vibration Control," *Sensors and Actuators A (Physical)*, Vol. 135, No. 2, April 2007, pp. 801–810. doi:10.1016/j.sna.2006.09.020

[5] Nutting, P. G., "A New General Law of Deformation," *Journal of the Franklin Institute*, Vol. 191, 1921, pp. 679–685. doi:10.1016/S0016-0032(21)90171-6

[6] Bagley, R. L., and Torvik, P. J., "A Theoritical Basis for the Application of Fractional Calculus to Viscoelasticity," *Journal of Rheology (New York)*, Vol. 27, No. 3, 1983, pp. 201–210. doi:10.1122/1.549724

[7] Li, Y., Xu, M., "Hysteresis and Precondition of Viscoelastic Solid Models," *Mechanics of Time-Dependent Materials*, Vol. 10, No. 2, 2006, pp. 113–123. doi:10.1007/s11043-006-9013-2

[8] Sunny, M. R., Kapania, R. K., Moffitt, R. D., and Mishra, A., "A Modified Fractional Calculus Approach to Model Hysteresis," *Journal of Applied Mechanics*, Vol. 77, No. 3, 2010, Paper 031004. doi:10.1115/1.4000413

[9] Preisach, F. Z., "Uber die Magnetische Nachwirkung," *Zeitschrift für Physik*, Vol. 94, 1935, pp. 277–302. doi:10.1007/BF01349418

[10] Everett, D. H., and Whitton, W. I., "A General Approach to Hysteresis," *Transactions of the Faraday Society*, Vol. 48, 1952, pp. 749–757. doi:10.1039/tf9524800749

[11] Cornejo, D. R., and Missell, F. P., "Application of the Preisach Model to Nanocrystalline Magnets," *Journal of Magnetism and Magnetic Materials*, Vol. 203, Nos. 1–3, 1999, pp. 41–45. doi:10.1016/S0304-8853(99)00182-1

[12] Roshko, R. M., and Huo, D. L., "A Preisach Characterization of the Barkhausen Spectrum of a Canonical Ferromagnet $SrRuO_3$," *Physica B: Condensed Matter (Amsterdam)*, Vol. 306, No. 1–4, Dec. 2001, pp. 246–250. doi:10.1016/S0921-4526(01)01012-2

[13] Vandenbossche, L., Dupr, L., and Melkebeek, J., "Preisach-Based Magnetic Evaluation of Fatigue Damage Progression," *Journal of Magnetism and Magnetic Materials*, Vol. 290-291, No. 1, April 2005, pp. 486–489. doi:10.1016/j.jmmm.2004.11.508

[14] Guyer, R. A., McCall, K. R., Boitnott, G. N., Hilbert, L. B., and Plona, T. J., "Quantitative Implementation of Preisach–Mayergoyz Space to Find Static and Dynamic Elastic Moduli in Rock," *Journal of Geophysical Research*, Vol. 102, No. B3, March 1997, pp. 5281–5293. doi:10.1029/96JB03740

[15] Schiffer, A., and Ivanyi, A., "Preisach Distribution Function Approximation with Wavelet Interpolation Technique," *Physica B: Condensed Matter (Amsterdam)*, Vol. 372, Nos. 1–2, Feb. 2006, pp. 101–105. doi:10.1016/j.physb.2005.10.026

[16] Yunhe, Y., Xhengchu, X., En-Bing, L., and Nagi, N., "Analytic and Experimental Studies of a Wavelet Identification of Preisach Model of Hysteresis," *Journal of Magnetism and Magnetic Materials*, Vol. 208, No. 3, Jan. 2000, pp. 255–263. doi:10.1016/S0304-8853(99)00590-9

[17] Mayergoyz, I. D., *Mathematical Models of Hysteresis and Their Applications*, Elsevier Series in Electromagnetism, Elsevier, New York, Aug. 2003.

[18] Cross, R., Krasnosel'skii, A. M., and Pokrovskii, A. V., "A Time-Dependent Preisach Model," *Physica B: Condensed Matter (Amsterdam)*, Vol. 306, No. 1–4, Dec. 2001, pp. 206–210. doi:10.1016/S0921-4526(01)01005-5

[19] Sunny, M. R., and Kapania, R. K., "A Hysteresis Compensator Based on a Modified Dynamic Preisach Model for Conductive Polymer Nanocomposites," *IUTAM Symposium on Multi-Functional Material Structures and Systems*, Springer (to be published).

[20] Mayergoyz, I. D., "Hysteresis Models from the Mathematical and Control Theory Point of View," *Journal of Applied Physics*, Vol. 57, No. 8, 1985, pp. 3803–3805. doi:10.1063/1.334925

[21] Tan, X., and Bennani, O., "Fast Inverse Compensation of Preisach-Type Hysteresis Operators Using Field-Programmable Gate Arrays," *American Control Conference*, Seattle, WA, June 2008.

N. Wereley
Associate Editor